FARADAY

Solvation and catalyst–substrate superstructure of a tungsten tris(dithiolene) complex dissolved in water–acetone

A molecular dynamics model calculation

Jannis Samios,*[a] Dimitris Katakis,*[b] Dimitris Dellis,[a] Emmanouel Lyris[b] and Christine-Anne Mitsopoulou[b]

[a] *Laboratory of Physical Chemistry, Department of Chemistry, University of Athens, Panepistimiopolis, 157 71 Zografou, Greece*
[b] *Laboratory of Inorganic Chemistry, Department of Chemistry, University of Athens, Panepistimiopolis, 157 71 Zografou, Greece*

Received 13th May 1998, Accepted 27th July 1998

The intermolecular interactions of the catalyst tris(1,2-ethylenedithiolate-*S*,*S*′)tungsten, $W(S_2C_2H_2)_3$, with the molecules of a 25 : 75 water–acetone mixed solvent, are examined by statistical mechanical methods, and specifically by a molecular dynamics (MD) technique, using charge distributions obtained by extended Hückel calculations. The results are presented in the form of pair correlation functions (PCF), and show that an average of up to three water molecules come close to the sites of the catalyst, whereas the acetone molecules form an open cage at a somewhat longer distance. The supramolecular structure around the catalyst is asymmetric, and is examined in the two characteristic geometries corresponding to the D_{3h} and C_{2v} symmetries which the 'tris(dithiolene)' molecule transiently assumes during its fluxional metamorphoses in solution. At large distance (large values of the correlation parameter r) the system is homogeneous. Yet, at nanometer distances the symmetry breaks down, and the system becomes highly asymmetric with differentiation (selectivity) in space. The mobility of the water and acetone molecules, close to the catalyst, was also studied by estimating the translational self-diffusion coefficients D_{wat} and D_{acet} from the center of mass linear velocity correlation functions. The results show that the water molecules are more mobile than the acetone molecules, which is the opposite of what happens without the catalyst.

Introduction

For a thorough investigation of homogeneous catalysis it is necessary to consider both the molecular and supramolecular characteristics of the system. Included in the former are such features as composition, structure and electron distribution of the catalyst and the intermediates. The supramolecular features on the other hand include intermolecular interactions between the catalyst and the substrate, and solvent effects. The study of these supramolecular features, *i.e.* of the dynamics of the catalyst–substrate–solvent interactions is a necessary supplement to the intramolecular effects, if we want to understand the process as a whole. The recognition of the need to combine molecular and intermolecular effects in order to gain a deeper understanding of events, may be the motivation behind the work of Roald Hoffmann and his collaborators, when they try to understand the stacking of dithiolenes after performing simple extended Hückel calculations on the molecules[1] or when using the molecular orbitals of the chemist to describe solid state physics.[2] Here, we do not attempt a comprehensive review of all efforts to combine molecular and intermolecular aspects. The particular investigator is only mentioned as a prominent example.

In this report we apply this combined molecular and intermolecular approach to homogeneous catalysis, using simple extended Hückel (EH) calculations[3] and a statistical mechanics approach *via* molecular dynamics (MD) simulations.[4]

The catalyst studied is a 'tris(dithiolate)'. Dithiolates are well known catalysts and photocatalysts.[1,5,6] The thermal catalytic activity of these compounds has been demonstrated in the reduction of water to dihydrogen with the free radical $MV^{\bullet+}$ as the electron donor[5] or with the electrons supplied electrochemically.[6] Both square planar $M[S_2C_2R_1R_2]_2$ and trigonal prismatic $M[S_2C_2R_1R_2]_3$ dithiolenes can be used for the thermal or electrochemical catalysis.[7]

'Tris(dithiolates)' as photocatalysts have been studied in the water splitting reaction.[8] In this reaction the dithiolene absorbs the light energy, transfers it to water and it also acts as a thermal catalyst in the formation of hydrogen and oxygen. Only three non-symmetric 'tris(dithiolates)' $W[S_2C_2(H)(MeOPh]_3$, $W[S_2C_2(Ph)(p\text{-}MeOPh)]_3$ and $W[S_2C_2(Ph)(p\text{-}Me_2NPh)]_3$ are known[8] to be active in this case, and at the same time to have the necessary thermal and photochemical stability.

To start with, we concentrate directly on the thermal and/or electrochemical catalysis and only indirectly on the photochemical. The latter will be (hopefully) examined in a future paper. For the thermal case, (H_2 from H_2O with an electron donor), the catalysis is generally thought to involve two electron transfer steps, two proton oxidative addition steps, and an H_2 elimination reaction (Scheme 1).

The kinetics give some information about the rate determining step, but there are still several questions that need elucidation, such as: what are the precursors of the species formed in this sequence, how are the reacting molecules arranged in space, and what are the possible interactions between them; in short, what is the dynamic supramolecular structure prior to the commencement of the reaction sequence, and how critical is this arrangement for the reaction?

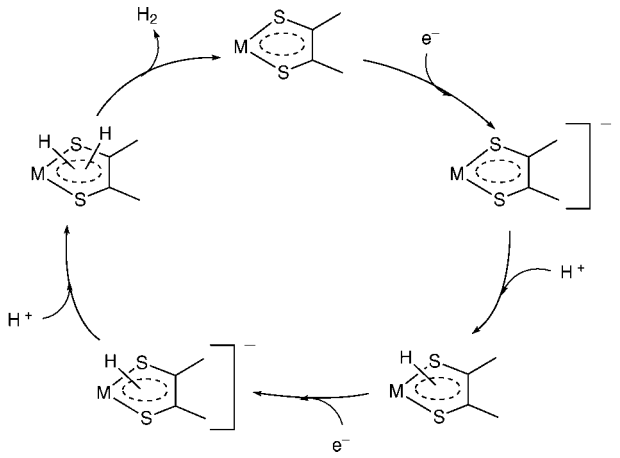

Scheme 1†

On the molecular level there is not enough information either about the species formed: whether the proton is added on the metal or on sulfur

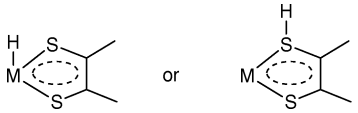

and whether the hydrides are formed by direct transfer to the catalyst or by successive transfer to the solvent (H_2O) and then to the catalyst. The second proton addition can again be on the metal or on sulfur, and there are several possibilities for H_2 elimination, such as:

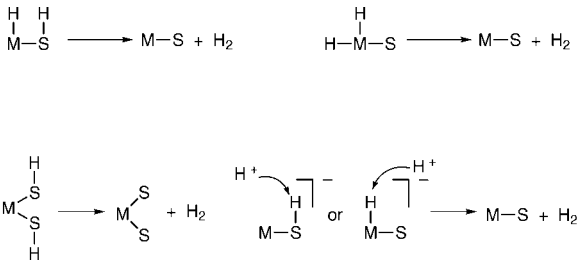

The molecular characteristics of 'tris(dithiolates)' have been studied quite extensively.[7] Regarding the supramolecular aspects, some evidence has been mentioned,[8] indicating that supramolecular formation of a given compensation precedes the catalytic process. Here we begin an attempt for a systematic investigation, in order to obtain a picture of these dynamic supramolecular clusters by classical statistical mechanical computations (molecular dynamic simulation), based on molecular characteristics obtained quantum mechanically. We consider a somewhat simplified three-component system containing the trigonal prismatic tris(1,2-ethylenedithiolate-*S*-*S*′)tungsten, $W[S_2C_2H_3]_3$, dissolved in a mixed water–acetone (25 : 75) solvent.

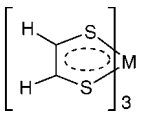

The catalyst is insoluble in water but soluble in non-aqueous solvents. On the other hand, we require as much water as possible, since it is the reactant. The 25 : 75 water–acetone solvent mixture has enough acetone to make the catalyst soluble and the system homogeneous, and enough water for good yields of photochemical splitting[8] or thermal dihydrogen production.[5]

We are interested in the average number of water molecules coming close to the catalyst, how much they approach, and if possible what are the preferable orientations. We also try to assess the role of acetone in this process and establish the composition and average intermolecular structure of the supramolecular system, which eventually leads to the catalytic process. We are also interested in the mobility of the solvent molecules around the catalyst, and here we give estimates of the self-diffusion coefficients for water and acetone.

Methods, potentials and parameters

The molecular dynamics (MD) simulations were carried out in microcanonical ensemble (NVE) with one $W[S_2C_2H_2]_3$ molecule dissolved in a mixture consisting of 64 water and 191 acetone molecules (the mole fraction of water is 0.25) in a cubic box with periodic boundary conditions. The system molar volume, 59.05 cm^3 mol^{-1}, is the experimental[9] one of the 25 : 75 water : acetone mixture at 298 K. This is justified by the high dilution of the solutions. The molecules are treated as rigid rotors. The initial configuration of the molecules was specified by placing the catalyst molecule in the center of the simulation box with the solvent molecules randomly distributed around the catalyst taking care to avoid possible overlap between catalyst and solvent atoms as well as between solvent atoms. In addition, attention was paid so that the molecules of the solvent component with the smaller concentration (H_2O) are initially uniformly diluted among the acetone molecules. Also, the initial orientation of each molecule was selected randomly. The molecular interactions between the various species in the system were of the type site–site Lennard-Jones (LJ), supplemented by electrostatic terms in the form of partial charges localized on the atoms of the molecules. Long range electrostatic interactions were treated using the Ewald summation technique. A full cut-off radius ($r_C = L_{BOX}/2$) was applied to all interactions between the species of the system.

$$U_p = \sum\sum\left[4\varepsilon_{ij}\left[\left(\frac{\sigma_{ij}}{r_{ij}}\right)^{12} - \left(\frac{\sigma_{ij}}{r_{ij}}\right)^{6}\right] + \frac{1}{4\pi\varepsilon_0}\frac{q_i q_j}{r_{ij}}\right]$$

The potential parameter values are given in Table 1.

The orientation of the molecules have been formulated using a quatenion interpretation, which offers the possibility that the equations of motion may be free of singularities. The equations of motion are solved using a leapfrog algorithm.[10] In order to achieve the most stable results, we have tested several integration time steps dt. By comparing the predicted results we were able to conclude that a time step of 2×10^{-15} s ensures stability of the calculated energy and momentum. The number of equilibrium time steps was approximately 500 000. In order to obtain accurate statistics, each production run after equilibrium was extended to *ca.* 1000 ps. During the simulation and after the equilibrium procedure, the temperature was close (± 8 K) to the initial temperature. The total energy drift was lower than 1 in 10^4 for the whole simulation. The macroscopic thermodynamic properties and the time dependent autocorrelation functions corresponding to the single molecule dynamical properties were obtained. Finally, all the relevant site–site pair distribution functions (PDFs) of the system were obtained and analyzed.

Potentials for the cross-interaction were handled with the Lorentz–Berthelot combining rules:

$$\sigma_{ij} = \frac{\sigma_{ii} + \sigma_{jj}}{2}, \quad \varepsilon_{ij} = (\varepsilon_{ii} \cdot \varepsilon_{jj})^{1/2}$$

The water–water interactions were approximated by using the SPC potential model.[11] For acetone, a four-site model was used, starting from the gas-phase geometry and a published charge distribution.[12] This charge distribution yields a dipole

† Only one dithiolenic ring is depicted and only the changes in overall charge from that of the original form of the catalyst.

Table 1 Parameters of the potential and the charges for the D_{3h} and C_{2v} symmetries of $W(S_2C_2H_2)_3$, and for acetone and water molecules

	$WS_6C_6H_6$[a]						Acetone			Water	
	W	S(a)	S(b)	C(a)	C(b)	H	CH_3	C	O	H	O
εk_B^{-1}/K	281.0	183.0	183.0	51.2	51.2	8.60	85.0	52.84	105.7	0	78.23
σ/Å	3.790	3.520	3.520	3.350	3.350	2.81	3.86	3.75	2.960	0	3.166
q^b/e	1.824	−0.262		−0.066		0.024	−0.032	0.566	−0.502	0.41	−0.82
	1.894	−0.24	−0.291	−0.059	−0.069	0.024					

[a] S(a), S(b), C(a) and C(b) refer to the sulfurs and carbons of structure **B**. [b] The first line for q/e refers to D_{3h}, the second to C_{2v}. The charges q/e are given per atom of the molecule.

amount for the acetone molecule of 2.7 D,‡ compared with the gas-phase value of 2.9 D. The LJ, C–O and O–O parameters of the ketone groups were also taken from the literature,[13,14] but the methyl group parameters were adjusted slightly to yield a more reasonable calculated pressure for the water–acetone simulation. For the $W[S_2C_2H_2]_3$ molecule such potentials are not available in the literature. However, we have tested various parameters. For the S, C and H atoms, the potential parameters of similarly bonded systems were used.[15] In the case of the W atoms the short range LJ potential parameters are not available either. At this stage, for the W–W potential parameters we have used the Xe–Xe parameters,[16] since W^{VI},[7] is isoelectronic with Xe. To our knowledge, a similar procedure has been applied in the construction of the potential model of other molecular liquid systems which have been simulated successfully.[17] Moreover, MD trial runs made with different LJ parameters, σ within the range 3–4 Å and ε/k_B within the range 200–400 K, for the W–W interactions, showed negligible change in the catalyst–water–acetone thermodynamic and structural properties.

The translational motion of the solvent molecules around the catalyst was studied by calculating the corresponding time correlation functions (TCF) of the center of mass (COM) linear velocities $C_v^{wat}(t)$ and $C_v^{acet}(t)$, given by:

$$C_v^x = \frac{\langle \boldsymbol{v}_x(0) \cdot \boldsymbol{v}_x(t) \rangle}{\langle \boldsymbol{v}_x(0)^2 \rangle} \qquad x = H_2O, \text{ acetone}$$

The self-diffusion coefficients D_{wat} and D_{acet} are evaluated by obtaining the time integrals, of the non-normalized TCFs. The space around the catalyst was divided into two regions. The first starts from the center of the catalyst molecule (the W atom) and extends to a radius of 7 Å, [the position of the second minimum in the $g_{W-wat}(r)$]. The second is a spherical shell with $r_{min} = 7$ Å to $r_{max} = r_C$. For each region corresponding linear velocity TCFs $C_v^x(t)$ were evaluated using long statistics (*ca.* 250 ps).

The localized charges on each atom of the $W[S_2C_2H_2]_3$ molecule obtained using EH calculations are given in Table 1. The molecular geometries used in the calculation are trigonal prismatic with D_{3h} and C_{2v} symmetry. The bond distances and angles were obtained from published crystal structures[18] and are W—S 2.33 Å, S—C 1.70 Å, C—C 1.30 Å, C—H 1.10 Å, S—W—S 82°, W—S—C 108°, S—C—C 121°, S—C—H 120°. The program used for the EH calculation is CACAO.[3] The program calculates successively the distance matrix, the overlap matrix, the input Hückel matrix H, using the modified Wolfsberg–Helmholz expression $[H_{ij} = CS_{ij}[(1 + \Delta)H_{ii} + (1 - \Delta)H_{jj}]/2]$, the eigenvalues of the energy and the total energy, MO's coefficients, and performs a Mulliken population analysis, from which the charges on the atoms are obtained.

Dithiolenes undergo a *cis–trans* isomerization[7] with an activation energy of 13.6 kcal mol^{-1}; the trigonal prism is not rigid. The isomerization has been postulated to occur by an electric switch-like rotation of one of the dithiolenic rings:

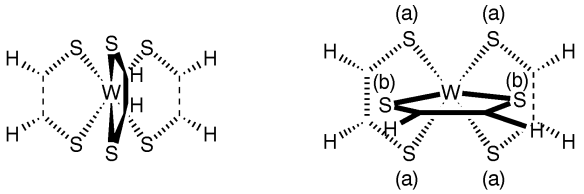

The distribution of charges for **A** and **B** is different as can be seen in Table 1. Two independent MD calculations were carried out for these two geometries under the same thermodynamic conditions.

Results and discussion

Intermolecular structure

The intermolecular structures of the simulated system based on the charge distribution obtained by the EH calculations, are presented in the form of pair correlation functions (PCFs) (Fig. 1–3). The correlation radius r refers to the distance of the

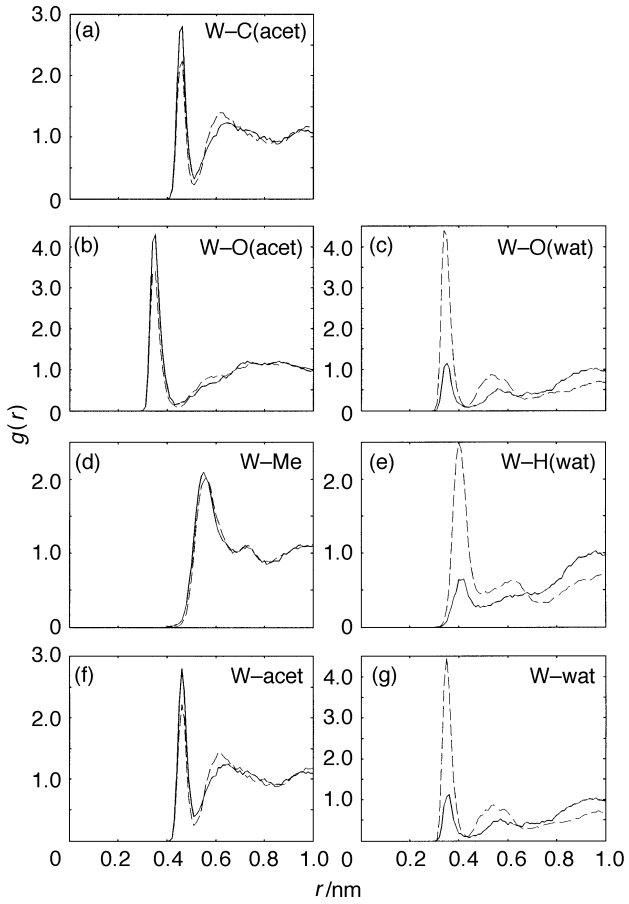

Fig. 1 Pair correlation functions from W to the center of mass of water and acetone, and to different sites of these molecules: (——) configuration **A**, (- - -) configuration **B**.

‡ D ≈ 3.33564 × 10^{-30} C m.

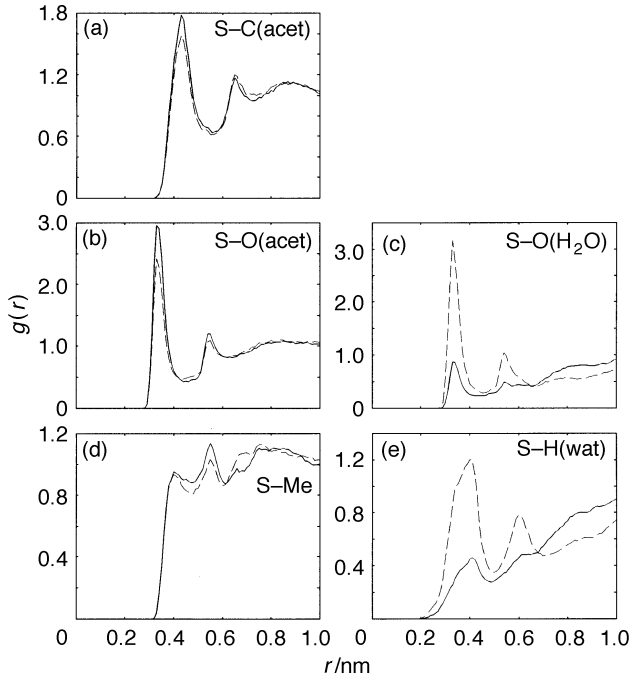

Fig. 2 Pair correlation functions from S to the center of mass of water and acetone, and to different sites of these molecules: (——) configuration **A**, (– – –) configuration **B**.

various sites (atoms) of the catalyst from the COM of the water and acetone molecules, and also from the different sites (atoms) of these molecules. The acetone CH_3 groups are considered as united interaction sites located at the carbons.

Note that water is one of the components of the solvent, but it is also the substrate of the catalytic reactions considered.

For comparison we estimated the PCFs of water–water and acetone–acetone, which correspond to long distances from the catalyst. They were found to agree (in the position and height of the PCFs r maxima) to those obtained for the pure 25 : 75 mixture[13] and it is not considered necessary to reproduce them here.

From Fig. 1 it is seen that the water molecules tend to accumulate closer to W [Fig. 1(g)] than the acetones [Fig. 1(f)]:

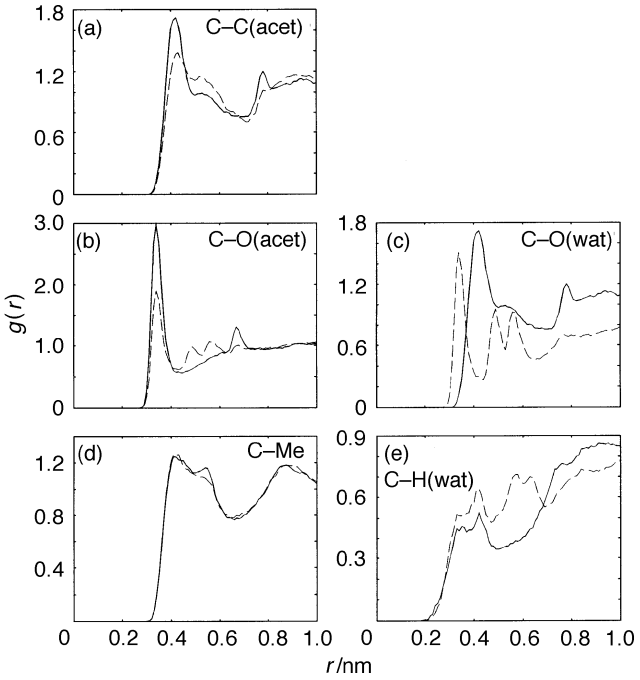

Fig. 3 Pair correlation functions from C to the center of mass of water and acetone, and to different sites of these molecules: (——) configuration **A**, (– – –) configuration **B**.

the first peak of the COM PCF W–H_2O is located at sufficiently shorter distance than the first peak of the COM W-acetone function. The bulk of the acetone molecules form an open cage, in which the catalyst and the substrate can be considered to be dynamically trapped. This restricted region can be regarded as the active site (region) of the catalytic system. The carbonyl oxygens of the acetones have some tendency to orient towards the reactive region. This is supported by the observation that the first peak of the W–O(acet) function is located at shorter distance ($\cong$3.7 Å) compared to the first peaks of the other functions. On average the acetone layer seems to be followed by a water–acetone layer, as indicated by the second peak, in Fig. 1(c), (e), (g), but after that the correlation first goes through a shallow minimum and then converges smoothly to one, it tends to that of the pure solvent (see above). It should be recalled that the averaging considered here is over time, but also round the molecule, which is by no means spherical.

It is also seen from Fig. 1(c), (e), (g), that the position of the maxima in $g(r)$ for W to water COM or the water atom sites are not affected by the 90° rotation of one of the rings (**A** and **B** conformations). The peak intensity, however, and consequently the surface under the peak for conformation **B** is larger, indicating that more water molecules can be accommodated within the inner restricted region. On the contrary the number of acetone molecules forming the cage 'walls' is not affected by the rotation.

The supramolecular geometry allows, even favours, interactions of water with W or with S, but it also allows for a collective interaction with both. With the accuracy of the EH calculations, reliable quantitative estimates of the relative values (attraction to W or S) cannot be made. It is then perhaps safer to assume at this stage, recalling also that the system is dynamic, that both interactions (to W and to S) are possible. From Fig. 2 we can see further that some peaks become double in height or wider, which may reflect the fact that there are three pairs of sulfurs in the catalyst molecule, and also the fact of the relatively low symmetry of the charge distribution. A similar remark can be made for Fig. 3.

The dithiolene carbon–water (Fig. 3) correlation is the only case where the 90° rotation affects also the position of the maximum; the molecules of water seem (on average) to come closer to these carbons when one of the rings is rotated by 90°. The distances between the six sulfur atoms (two from each dithiolenic ring) is more or less equal.[7] Thus upon rotation by 90° of one of the rings, the prismatic geometry, focusing on sulfur atoms, is retained:

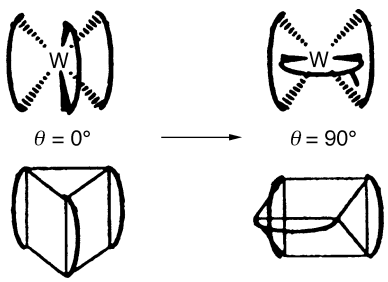

but focusing on the carbon atoms is not.

The coordination numbers up to the first maximum of each PCF for the simulations of configurations **A** and **B** are collated in Table 2.

Since the system is dynamic, a variable number of solvent molecules is coordinated to the catalyst. This number depends on the change in the configuration of the catalyst during its *cis–trans* isomerization. For structure **B** the coordination numbers for water are higher. The W–S distance is 2.33 Å, the distance between W and the carbons of the chelate rings is 3.281 Å, and the C–H distance is 1.10 Å. If we take the hydrogen as the limit of the first coordination sphere, we see from

Table 2 Coordination number of various radial distribution functions as a function of the maximum integration distance, for the D_{3h} (first line) and the C_{2v} (second line) symmetries

	r_{max}/nm 0.2	0.3	0.34	0.38	0.42	0.46	0.5	0.6
$g_{W-Water}$			0.2	1.4	1.6	1.7	1.8	2.1
			0.6	3.0	3.2	3.4	4.2	7.0
$g_{Water-Acetone}$			0.1	1.6	2.2	3.5	5.5	8.4
			0.1	1.0	1.9	3.1	4.7	7.8
$g_{W-Acetone}$						1.2	3.4	5.6
						1.1	2.7	5.6
$g_{W-O(Water)}$			0.2	1.5	1.6	1.7	1.8	2.1
			1.0	3.1	3.3	3.4	4.2	7.0
$g_{W-H(Water)}$				0.4	0.9	1.5	1.8	2.0
				0.9	2.4	3.5	4.3	6.2
$g_{S-O(Water)}$			0.4	1.1	1.2	1.3	1.4	2.2
			1.2	2.5	2.8	3.0	3.6	6.3
$g_{S-H(Water)}$			0.2	0.6	0.8	1.2	1.4	2.1
		0.1	0.5	1.4	2.2	2.9	3.5	5.5
$g_{C-O(Water)}$			0.4	1.1	1.1	1.2	1.4	1.9
			0.5	1.2	1.4	1.8	3.0	5.6
$g_{C-H(Water)}$		0.1	0.3	0.6	0.8	1.1	1.4	2.0
		0.1	0.3	0.8	1.2	1.7	2.5	4.8
g_{W-CH_3}							1.2	7.1
							0.6	6.9
$g_{W-C(Acetone)}$						1.5	3.4	5.6
						1.4	2.7	5.6
$g_{W-O(Acetone)}$					0.4	2.6	3.4	6.7
			0.7	2.4	2.6	2.8	3.2	5.8

Table 2 that there are only up to three water molecules within this sphere, on average (in time and around the molecule). One of them penetrates deeper into the 'tris(dithiolate)', closer to tungsten, and one or two more remain at a longer distance. Acetone is at a considerably greater distance, from what can be considered as the second coordination sphere. There is a considerable increase in the coordination number of the catalyst, up to nine if we consider only water molecules and the sulfurs. This consideration seems to be necessary in this case. An increase in 'coordination number' had to be evoked,[8] in order to explain the experimental data in photocatalysis.

It is also seen that the water molecules tend to orient their oxygen, rather than the hydrogens towards W. Supporting evidence for this is the observation that the position of the first peak in the W–O(H_2O) function ($\cong$3.6 Å) is located at shorter distance than that of the W–H(H_2O) function ($\cong$4 Å). What is also interesting is that the water oxygens seem to come close to the other sites of the dithiolenic ring too, the Ss and the Cs [Fig. 2(c), 3(c)]. For the water hydrogens there seems to be some preference towards S and C [see Fig. 2(e), 3(e)]. Thus, the overall picture emerging is that the catalyst and, on average, up to three water molecules, are confined within an acetone cage form, between the 'paddles' on the prismatic catalyst and that the water molecules have access to any of the ring atoms.

Some evidence for the local structure around the catalyst indicated by the PCFs is also provided by inspecting arbitrary snapshots of the molecular configurations, two of which are depicted in Fig. 4 and 5. Fig. 4 is a snapshot of the catalyst and its immediate environment, which includes only water molecules, which are arranged quite irregularly around the catalyst, preferably in the space between rings, but by no means completely randomly. Another snapshot, on a larger scale, is given in Fig. 5, where it is clear that there are channels (indicated by arrows) for the penetration of the water molecules. The streams of the water molecules leading to tungsten, are not necessarily straight, and the orientation is not that expected for hydrogen bonded water molecules. The catalyst seems to act as a structure (hydrogen bonding) breaker. As we can see below, this observation is in accordance with the mobility of the water and acetone molecules around the catalyst estimated in the framework of this study.

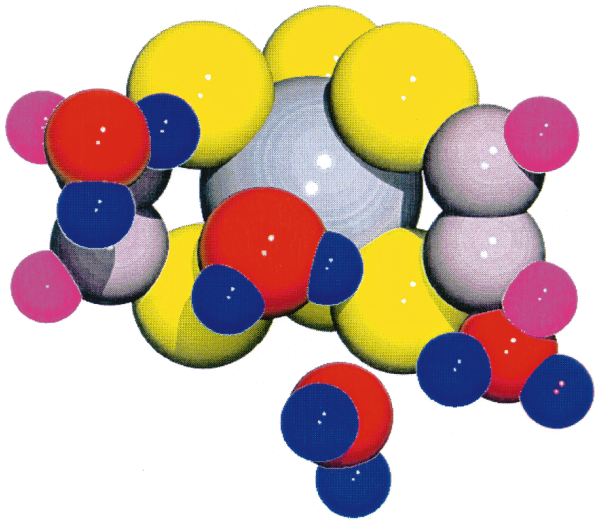

Fig. 4 Snapshot of the catalyst (confirmation **A**) and its immediate environment. W: light gray, S: yellow, C: dull pink, H_{CAT}: bright pink, O_{WAT}: red, H_{WAT}: blue (Water molecules on the rear of the catalyst, have been clipped away for reasons of clarity.)

It is also useful to note that all the activity seems to take place in the space between the dihedral angles of the catalyst molecule. The two trigonal faces of the prism do not seem to be involved, and do not seem to interact with water molecules.

It is also obvious from Fig. 1 and Table 2 that at somewhat larger distances acetone molecules form a second coordination sphere ('wall'), which, however, is not spherical; a segment of this 'wall' is marked in Fig. 5 by a green line. Other segments contain also water molecules. The main forces combining to form the acetone cage are van der Waals forces between acetone molecules, electrostatic attraction between acetone carbonyl oxygens and the positive sites of the catalyst (mainly W), and (probably) diple–dipole interactions with water molecules.

The supramolecular structure of the catalyst–substrate complex, as it has emerged from the results, regarding the number and positions of the water and acetone molecules can

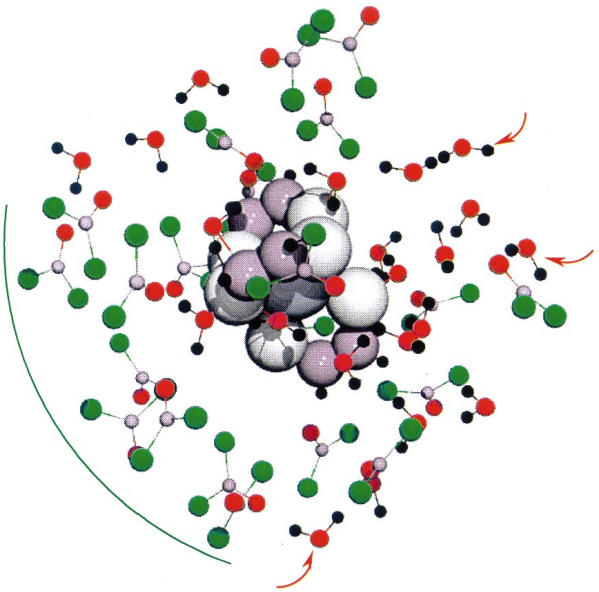

Fig. 5 Snapshot at larger distances, where there are acetone molecules. The arrows indicate water paths. Green line: part of acetone cage wall; catalyst: tungsten is dark gray in the middle of the molecule, sulfurs are light gray, carbons are dull pink, hydrogens are black; water molecules: oxygens are red and hydrogens are black; acetone molecules: methyl groups are green, carbonyl carbons are dull pink and carbonyl oxygens are red.

be characterised as fuzzy and dynamic. This is probably related to the fact that only electrostatic and dispersion forces are considered. Covalent bonding, in particular, was not one of the factors taken into account in the simulation. Also the disorder of the model must be related to the fact that the catalyst used has several active sites, has no rigid sterochemical structure in solution (is fluxional) and has rather low symmetry, especially when symmetry is considered in relation to solvent and substrate molecules. Thus, it seems that even in a homogeneous system such as this, local and/or temporary asymmetries characterise the dynamics of the reaction.

Generally, when we try to establish the relationship between structure and reactivity, the molecular structures (including those of the intermediates) are specific, even rigid. In the case we investigate here, there is fluxionality: change of the average shape of the catalyst molecule itself during some vibrational mode.[7] The simulation was performed for two specific rigid geometries, which however correspond to two extreme positions during the change of the shape. The calculations then showed that these extremes give quite different results. Thus, it is clearly shown that it is not only the idealized geometry (trigonal prismatic in this case), but also the changes it undergoes during the reaction (in this case the fluxionality of the catalyst) that affect the approach of the reactant molecules and therefore the catalytic reaction. Thus a more realistic picture is obtained, since catalysis requires mobility and pliability. Rigid structures are useful, but something more dynamic is needed for gaining a better understanding of catalysis.

It is interesting to note that in spite of the fact that the overall system considerd here is homogeneous, heterogeneous short range local dynamic structures are formed due to the presence of the catalyst molecule. By taking into account this finding and under the assumption that a similar local structure around the catalyst is formed in the catalytic system, we may assume that it could behave as a nano-minireactor. From this point of view the real system could also be regarded as a link between homogeneous and biphasic catalysis.

As implied in the Introduction a necessary process for the reduction of the water molecules is proton transfer to the catalyst. Indirect transfer first to another water molecule forming H_3O^+, and eventually to the catalyst is not considered; the solutions were not acidified, the protons were scarce, and the water molecules in the cage few and rather scattered, hence kinetically the indirect process is unlikely. Direct transfer on the other hand is largely determined by the proximity of the water hydrogens to the sites where the protons are transferred. By comparing the peaks of the various site–site correlation functions (Fig. 1–3) and the data in Table 2, we can argue that on average the water hydrogens tend to come closer to the rest of the dithiolate ring, rather than to the metal. Thus, although the formation of a metal hydride cannot be excluded, the simulations indicate that the reduction is more likely taking place at these other sites.

Solvent translational dynamics

By comparing the results of the TCFs $C_v^{wat}(t)$ of the two regions, the space around the catalyst has been divided, and we find that the regions show almost identical behaviour. A similar situation is obtained for the TCFs of the acetone molecules. For this reason we present only the results for the short range domain, which are illustrated in Fig. 6. The curves in this figure show the following qualitative behaviour. The TCF of the acetone molecules first goes through a shallow negative minimum and then converges to zero after approximately 1.3 ps. The TCF of the H_2O molecules goes more rapidly to negative values (in less than 0.2 ps) showing also a shallow anticorrelation region and then faster relaxation to zero. The time integral of each non-normalized TCF was

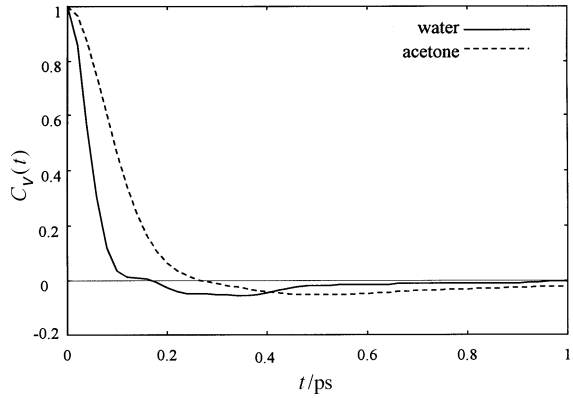

Fig. 6 Center of mass linear velocity correlation functions $C_v(t)$ for the H_2O (——) and acetone (– – –) molecules around the catalyst.

evaluated in order to obtain the self-diffusion coefficients D_{wat} and D_{acet}. The integration was carried out up to 1.5 ps and the results are as follows: for the H_2O molecules we obtain a value of $D_{wat} = 2.79 \times 10^{-9}$ m^2 s^{-1}, while for the acetone molecules a somewhat smaller value of $D_{acet} = 2.56 \times 10^{-9}$ m^2 s^{-1}.

In a pure (without catalyst) 25 : 75 water : acetone mixture at room temperature, NMR experiments yielded the values $D_{wat}^{exp} = 3.7 \times 10^{-9}$ m^2 s^{-1}, $D_{acet}^{exp} = 4 \times 10^{-9}$ m^2 s^{-1}, and MD studies the values $D_{wat}^{sim} = 2.32 \times 10^{-9}$ m^2 s^{-1}, $D_{acet}^{sim} = 2.72 \times 10^{-9}$ m^2 s^{-1}. In other words, in a pure 25 : 75 mixture experiments and simulation show that acetone is more mobile than water. A trace amount of the catalyst seems (theoretically) to make the water molecules more mobile in accordance with the suggestion that the catalyst acts as a hydrogen bonding structure breaker. This can be regarded as the first stage of the catalytic process.

Conclusions

Acetone molecules form segments of a 'wall' around the catalyst. The more mobile water molecules seem to cut through this wall, and form dynamic channels coming all the way to the tungsten center. The catalyst seems to increase the mobility of the water molecules relative to that of the acetone molecules.

The first coordination sphere contains only a few water molecules at variable distances from tungsten and at different angles around it; it contains no acetone molecules. Within this first coordination sphere the water molecules tend to orient with their oxygen towards W.

The catalyst–substrate activity seems to take place in the solid angles, between the dithiolenic 'paddles'. The fluxionality of the 'tris(dithiolates)' clearly affects their catalytic activity.

It is also impressive that, even in a homogeneous system, local heterogeneous structures are created because of the asymmetries in charge distribution.

Finally, it is important to mention at this point that on the basis of the various site–site PCFs obtained in this work, both the supramolecular and molecular arrangements seem to be highly asymmetric, and presumably this is what provides the driving force for the reaction. However, in order to reach a conclusion about this, a systematic investigation of the spatial orientational correlation functions would be very useful. Work on this problem and other properties of the system is in progress.

The authors wish to acknowledge the General Secretariat for Research and Technology (GSRT) of Greece for financial support under grants EPET II. The CPU time allocation on

CONVEX C3820 and on HP-735 cluster of the computing center of the University of Athens, Greece, is also gratefully acknowledged.

References

1 S. Alvarez, R. Vicente and R. Hoffmann, *J. Am. Chem. Soc*., 1985, **107**, 6253.
2 R. Hoffmann, *Solids and Surfaces*, VCH, New York, 1988.
3 C. Mealli and D. M. Proserpio, *J. Chem. Educ*., 1990, **67**, 399; J. H. Ammeter, H. B. Burgi, J. C. Thibeault and R. Hoffmann, *J. Am. Chem. Soc*., 1978, **100**, 3686.
4 M. D. Allen and D. J. Tildesley, *Computer Simulations of Liquids*, Oxford University Press, New York, 1987.
5 E. Hontzopoulos, E. Vrachnou-Astra, J. Konstantatos and D. Katakis, *J. Mol. Catal*., 1985, **31**, 327; C. Mitsopoulou, J. Konstantatos, D. Katakis and E. Vrachnou, *ibid*., 1991, **67**, 137.
6 A. Vlcek and A. A. Vlcek, *Inorg. Chim. Acta*, 1980, **41**, 123.
7 P. Falaras, C. A. Mitsopoulou, D. Argyropoulos, E. Lyris, N. Psaroudakis, E. Vrachnou and D. Katakis, *Inorg. Chem*., 1995, **34**, 4536; D. Argyropoulos, C. A. Mitsopoulou and D. Katakis, *ibid*., 1996, **35**, 5549; D. Argyropoulos, E. Lyris, C. A. Mitsopoulou and D. Katakis, *J. Chem. Soc*., 1997, 615.
8 E. Hontzopoulos, E. Vrachnou-Astra, D. Konstantatos and D. Katakis, *J. Photochem*., 1985, **30**, 117; D. Katakis, C. Mitsopoulou, J. Konstantatos, E. Vrachnou and P. Falaras, *J. Photochem. Photobiol. A: Chem*., 1992, **68**, 375; D. Katakis, C. Mitsopoulou and E. Vrachnou, *ibid*., 1994, **81**, 103; E. Lyris, D. Argyropoulos, C. A. Mitsopoulou, D. Katakis and E. Vrachnou, *ibid*., 1997, **108**, 51.
9 J. Timmermans, *Physico-chemical constants of binary systems in concentrated solutions*, Interscience, New York, 1960, vol. 2.
10 D. Fincham and D. E. Heyes, *Information quarterly of computer simulation of condensed phases*, Daresbury Laboratory, England, CCP5, Newsletter, N6, 1988; D. Fincham, *Information quarterly of computer simulation of condensed phases*, Daresbury Laboratory, England, CCP5, Newsletter N12, 1984, p. 47.
11 H. J. C. Berendsen, J. P. M. Postma, W. F. Vangusteren and J. Hermans, in *Intermolecular forces*, ed. B. Pullman, Reidel, Dordrecht, 1981.
12 C. A. Wellington and S. H. Khouwaiter, *Tetrahedron*, 1978, **34**, 2183.
13 M. Ferrario, M. Haughney, I. R. McDonald and M. L. Klein, *J. Chem. Phys*., 1990, **93**, 5156.
14 W. L. Jorgensen and L. J. Swemson, *J. Am. Chem. Soc*., 1983, **105**, 1407.
15 W. L. Jorgensen, *J. Phys. Chem*., 1986, **90**, 6379.
16 J. M. M. Roco, A. Caho Hernandez, S. Velasco and A. Medino, *J. Chem. Phys*., 1997, **107**, 4844 (see Table 1).
17 A. Luzar and D. Chandler, *J. Chem. Phys*., 1993, **98**, 8160.
18 A. E. Smith, G. N. Schrauzer, V. P. Mayweg and W. Heinrich, *J. Am. Chem. Soc*., 1965, **87**, 5798; R. Eisenberg and J. A. Ibers, *J. Am. Chem. Soc*., 1965, **87**, 3776; R. Eisenberg in *Progress in Inorganic Chemistry*, ed. S. J. Lippard, Wiley, 1970, vol. 112, p. 314.

Paper 8/03586E